Stony Brook University

Primary Aberrations: An Investigation from the Image Restoration Perspective

A Thesis Presented

By

Shekhar Sastry

to

The Graduate School

in Partial Fulfillment of the Requirements

for the Degree of

Master of Science

In

Electrical Engineering

Stony Brook University

May 2009

Stony Brook University

The Graduate School

Shekhar Sastry

We, the thesis committee for the above candidate for the Master of Science degree, hereby recommend acceptance of this thesis.

Dr Muralidhara Subbarao, Thesis Advisor
Professor, Department of Electrical Engineering.

Dr Ridha Kamoua, Second Reader
Associate Professor, Department of Electrical Engineering.

This thesis is accepted by the Graduate School

Lawrence Martin
Dean of the Graduate School

Abstract of the Thesis

Primary Aberrations: An Investigation from the Image Restoration Perspective

By

Shekhar Sastry

Master of Science

In

Electrical Engineering

Stony Brook University

2009

Image restoration is a very important topic in digital image processing. A lot of research has been done to restore digital images blurred due to limitations of optical systems. Aberration of an optical system is a deviation from ideal behavior and is always present in practice. Our goal is to restore images degraded by aberration. This thesis is the first step towards restoration of images blurred due to aberration. In this thesis we have investigated the five primary aberrations, namely, Spherical, Coma, Astigmatism, Field Curvature and Distortion from a image restoration perspective. We have used the theory of aberrations from physical optics to generate the point spread function (PSF) for primary aberrations. The important issue of a missing link

between depth and the amount of aberration has been addressed for a simple thin lens model. A simulation of blurring due to aberration is carried out. All the results have been documented and a brief analysis is presented where necessary.

Contents

List of Figures

List of Tables

Chapter 1

Introduction

The motivation for this thesis is our interest in the restoration of images blurred due to optical aberrations. Our brief investigation of restoration of different aberrations revealed a gap in understanding the theory and phenomenon of aberrations. This thesis attempts to fill such gap. This work will guide us to investigate the subject of restoration with more insight. Some of the questions that we have attempted to address are:

- What are the different kinds of aberrations; why and how do they occur?

- How are primary aberrations different from the more common defocus (or out-of-focus aberration)?
- How do primary aberrations vary with camera parameters and distance?
- Why do aberrations result in shift variant blurring? Etc.

Chapter 2 starts with different imaging models such as the pinhole camera model, the Gaussian imaging model and diffraction imaging model, and their properties. It is essential to understand the behavior of different imaging models before we attempt to understand aberration.

In Chapter 3, we will take a look, in detail, at different kinds of aberrations starting from tilt, defocus, to the five primary aberrations. The concept of aberration function is introduced and all of the aberrations are explained using this concept.

Chapter 4 and onwards deal with only the primary aberrations. Calculation of aberration coefficients is explained in Chapter 3. A set of equations is also given to calculate the aberration coefficients of a thin lens. Later in this chapter, behavior of aberrations with distance and the size of the aperture are dealt.

Chapter 5: Calculation of aberration point spread functions (PSFs) is illustrated in this chapter. The knowledge of aberration function and aberration coefficient is used to calculate the PSFs. A simple algorithm is given to calculate the aberration PSF, which we have followed to obtain the results included in this chapter

The shift variant model of blurring has been introduced in Chapter 6. Starting with Fredholm equation, shift variant nature of blurring is discussed. Examples of simulated shift variant blurring using aberration PSF are included.

Chapter 7 includes a summary of this investigation and highlights our learning. It concludes with the scope of this thesis.

Chapter 2

Imaging Models

A brief discussion of different kinds of imaging models is presented here. We begin with the simple pinhole camera model which forms ideal 2D image, and discuss Gaussian imaging model. Finally, diffraction imaging is described whose results will be used in further chapters.

2.1 The Pinhole camera model

A pinhole (a small opening on an opaque surface) tends to form a real or inverted image of an object, behind the surface. A ray originating at a point object and travelling through the small opening remains in its path and forms image of the point object anywhere behind the surface. Ideally, in a pinhole camera, every point in the image is in focus as rays traveling through the pinhole do not get deflected

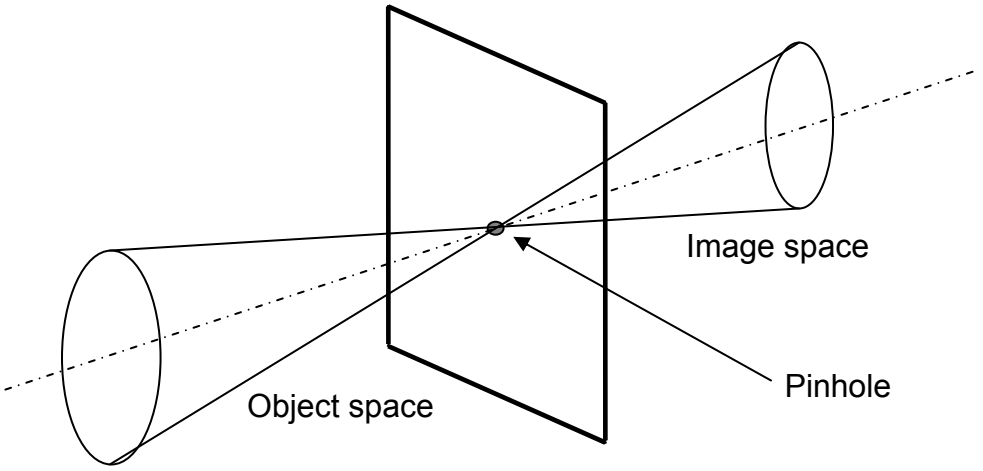

Figure 2.1: A diagram showing cone of light passing through a pinhole

2.2 A thin lens aperture model

A lens is an image forming element that contains many surfaces (usually part of a sphere, cylinder etc). It is different from pinhole as it has a much larger opening than the size of pinhole. The opening is referred to as the aperture of the lens. Lenses have the property of bringing rays that are parallel to the axis or normal at the center of the lens to focus. The point where such rays converge is called the focus. Any point object forms an image behind the lens where the chief ray meets the marginal rays, shown in Fig 2.2. The relation between the object and the image is given by the lens maker's formula

$$\frac{1}{l_1}+\frac{1}{l_2}=\frac{1}{f} \tag{2.1}$$

Where, l_1 is the object distance, l_2 is the image distance and f is the focal length (effective) of the lens.

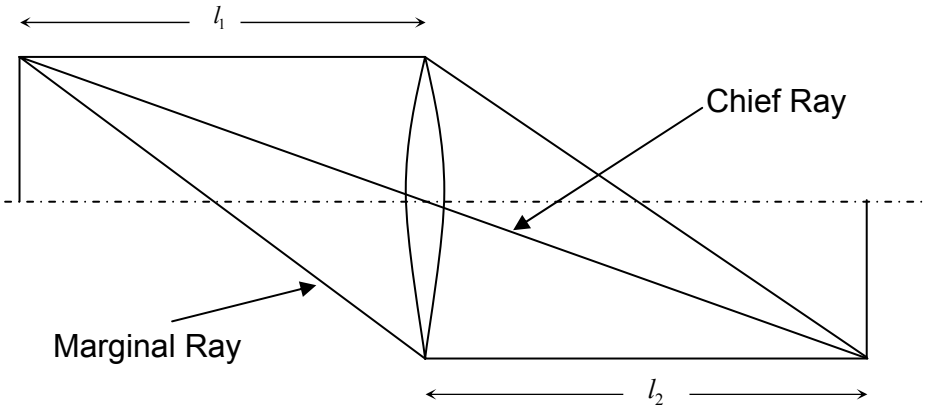

Figure 2.2: Gaussian imaging model

Gaussian imaging is when all rays from a point object are brought to focus. It is the ideal behavior of an image forming system and exists when all the rays from the object are parallel (nearly parallel) to the optical axis. If the image plane is at a distance different from that computed by the lens maker's formula, then the image is out of focus. This is commonly known as defocus and will be explained in detail later.

2.3 Diffraction imaging model

In this model we leave the confinement of geometric optics. Light is treated as a wave propagating in three dimensions. In vacuum, light travels like a spreading sphere around its origin and hence light incident on image forming system will be a part of such sphere. A perfect image forming system would invert a diverging spherical surface into a converging one so that a point image is formed behind the lens. The image is formed at a distance equal to the radius of sphere. So far we have explained Gaussian imaging in terms of waves.

An exit pupil in an imaging system is a virtual aperture or an image of the aperture stop seen from image space. If we trace rays from the source up till the exit pupil such that all rays travel same optical distance as the chief ray, then collection of such points is called a wavefront. Due to diffraction at the exit pupil, a wavefront never results in a point image; instead it is a set of rings around the Gaussian image point called Airy pattern. There are two important results due to this model:

1. The diffraction PSF of an imaging system is proportional to the modulus square of the inverse Fourier transform of the complex amplitude distribution at the exit pupil.

2. The diffraction image of a planar incoherent object is equal to the convolution of its Gaussian image and the PSF of the imaging system. We will use these two results in further chapters.

For illustration and proof of results refer [5]. A nice introduction to imaging models is given in [11].

So far three imaging models have been described. Ideally point light source should result in a point image. We will learn that due to some properties of imaging systems that is seldom the case. An image is said to be aberrated if it is different from the expected image given by imaging model. The diffraction imaging model is the reference model in our case.

Chapter 3

Aberrations

In the previous chapter we touched upon the phenomenon of aberrations. It was said that any behavior outside the diffraction imaging model (for our purposes) is called ‘aberration’. In this chapter let us delve more into the physics of aberration. First, we shall start with different kinds of aberrations describing each briefly.

Aberration is any deviation from an expected behavior. For example, if we choose diffraction imaging model as our primary model for imaging, then any deviation from that will be an aberration in most general sense. Refer [2] for details on different kinds of aberrations. For diffraction imaging and related topics, refer [5, 4]

3.1 Aberrations within paraxial optics

3.1.1 Tilt

It is a simple form of aberration. This occurs when the image of a point object is brought to focus on the Gaussian image plane but with a shift. If the expected location of image is at (X_i, Y_i) but was shifted to (X'_i, Y'_i) in the same plane then Tilt aberration is said to have occurred. This

usually happens if the surface of the imaging element is tilted with respect to the optical axis of the system.

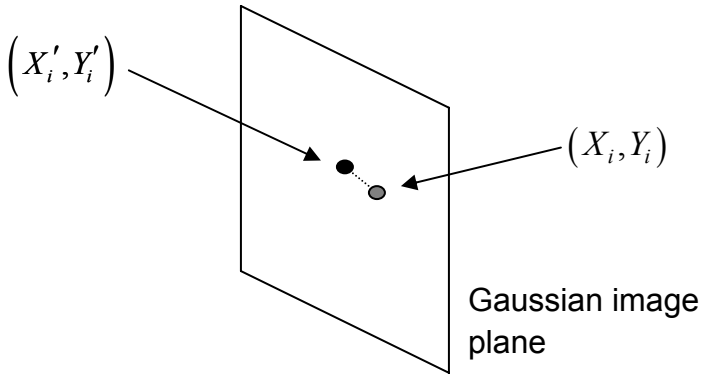

Figure 3.1: Shift in Gaussian image due to Tilt

3.1.2 Defocus Aberration

An image is observed on a plane behind the image forming system. The lens maker's formula gives the image distance in the Gaussian imaging model as

$$l_2 = \frac{l_1 f}{l_1 - f} \tag{3.1}$$

It is apparent from Eq. (3.1) that if the image distance is not the same as where the observation plane is, then the image is simply out of focus. The resulting image of a point object is not a point anymore, but it is smeared on the observation plane. As this is clearly a deviation from the expected behavior, the resulting image is aberrated and this aberration is called defocus. Such aberration can be corrected by moving the observation plane along the optical axis so that it is at a distance l_2, image distance, from the exit pupil.

These two aberrations exist even in most simplified models of image forming systems. It can occur even in paraxial optics assumption

unlike the primary aberrations which become prominent as paraxial assumption is relaxed.

3.2 Primary aberrations

There are five primary aberrations. They are Spherical, Coma, Astigmatism, Field Curvature and Distortion. In this section, we will describe each of the five primary aberrations in detail.

3.2.1 Aberration function

It is important to introduce something called as the aberration function before considering the aberrations. The aberration function is given by Eq. (3.2)

$$W(h',r,\theta) = {}_0a_{40}r^4 + {}_1a_{31}h'r^3\cos\theta + {}_2a_{22}h'^2r^2\cos^2\theta + {}_2a_{20}h'^2r^2 + {}_3a_{11}h'^3r\cos\theta \tag{3.2}$$

It is a function of three parameters h', r and θ:

h'	normalized image height in the observation plane
r	normalized height in pupil plane
θ	angle $\tan^{-1}(Y/X)$ in the pupil plane
${}_xa_{xx}$	peak aberration coefficient

Aberration function simply measures the total amount of aberration of the system for a given point object. As we can see, it is a sum containing five terms. The first term is the expression for spherical aberration and subsequent terms are for coma, astigmatism, field

curvature and distortion respectively. The pupil function, used to calculate PSF, is a function of W. It contains W in complex exponential term and describes the amplitude distribution in the pupil plane. We can use the result from diffraction imaging that the PSF is proportional to the inverse Fourier transform of the pupil function while calculating the PSF.

3.2.2 Spherical aberration

Spherical aberration is a property of imaging surfaces. It occurs whenever the incident wavefront at the lens does not match its surface i.e., if the wavefront is not complimentary to the surface of the lens then the emerging wavefront gets bent either too much or too little at the ends. This results in a ring like pattern around the point of Gaussian focus.

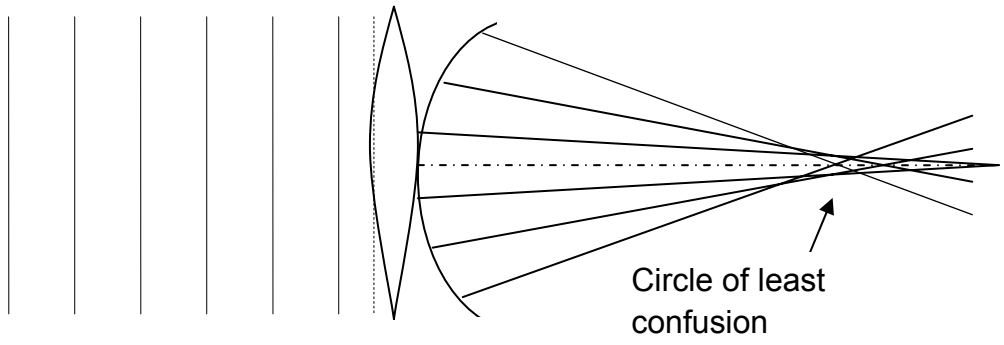

Figure 3.2: Spherical aberration

Imagine a wave emerging from a point far from the imaging system, so that its incident wavefront is almost planar. As it strikes a convex lens, the points near the axis meet the lens before the points off axis. The wavefront itself moves slowly near the center and it moves faster near the boundaries of lens. For the emerging wavefront, the points away from the axis emerge before others and hence they continue to travel faster. We can clearly visualize a planar wavefront getting bent towards the axis at each end causing spherical aberration, as shown in Fig. 3.2.

The expression for spherical aberration is given by ${}_0a_{40}r^4$. We can see that the aberration varies in fourth power of normalized height in the pupil plane. Also the expression is devoid of the term h'. Hence, it is apparent that spherical aberration is independent of object location on the image plane unlike any other primary aberration. It means that spherical aberration remains same across the image as long as the point object is located at the same distance from the imaging system. The amount of aberration depends on the aberration coefficient due to the point object under consideration.

This is the most important form of aberration to be considered for correction as it practically exists everywhere in the image. In optics, spherical aberration is known to be corrected by having surfaces with gradient refractive indices. For our purpose we measure the aberration with respect to the Gaussian image point. As we can see from the ray diagram there is a best focus point for spherical aberrated image, which is not Gaussian image point, called the circle of least confusion. If we measure the aberration with respect to this point then the aberration is called balanced spherical aberration. In practice, balanced aberrations are used (for optics), for us however classical aberrations are the norm.

3.2.3 Coma

Coma derives its name from the shape of the point image affected with this particular aberration. A point object gets shaped like a comet with sharpness decreasing along the axis of aberration. The occurrence of coma is due to the wavefront, from point object, being tilted with respect to the surface of lens.

Figure 3.3: Diagram showing comatic blur of a point object. The axis of aberration is vertical in the diagram.

The expression for coma from the aberration function is ${}_1a_{31}h'r^3\cos\theta$. As we can see coma varies in third power with respect to the normalized height in pupil plane r. It has $\cos\theta$ term which implies that coma is not symmetric about the optical axis. Lastly, we notice the term h'. This simply means that coma is absent near the center and it grows linearly as we move away from the optical axis on the observation plane. In other words, coma affects points that are off axis and grows linearly with the off axis distance of the point object.

Even for coma there are two forms; balanced coma and classical coma. For our purpose it is sufficient to understand and measure the classical coma, as it measures the aberration with respect to the Gaussian image point. The aberration coefficient for coma too depends on the object distance. We will consider this in detail when we describe aberration coefficients and PSFs.

3.2.4 Astigmatism

Astigmatism is another asymmetric aberration which affects off axis object points. The nature of this aberration is best explained by

considering rays. The plane containing the point object and the optical axis is called the meridional plane and a sagittal plane is the one perpendicular to it, both shown in Fig. 3.4. Astigmatism occurs when the rays in meridional plane and sagittal plane come to focus at different points. Usually, astigmatism is noticed by blur in a particular direction, for example, in the case of human eye we can notice that the horizontal edges are blurred whereas vertical edges are in focus (or vice versa).

The expression from aberration function for astigmatism is given as $_2 a_{22} h'^2 r^2 \cos^2\theta$. We notice that it is a function of $r\cos\theta$ in degree two. With the usual conventions, the term $r\cos\theta$ results in y_p coordinate of the pupil plane and hence should not be confused with defocus. Also it varies as h'^2, which means that astigmatism affects off axis points and the aberration is absent near the center. The severity of aberration grows in powers of two of the off axis distance. The aberration coefficient itself is independent of distance; it depends on the optical system's variables like Lagrange invariant, Power etc.

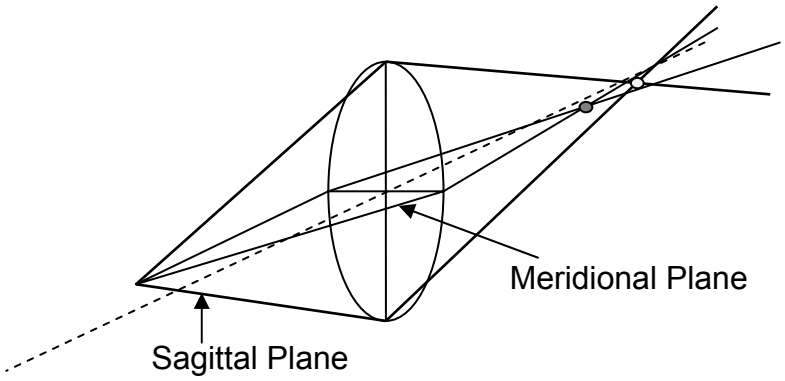

Figure 3.4: Sagittal and Meridional rays converging at different points

3.2.5 Field curvature

As the name suggests this aberration is due to curvature of field. It is because of the fact that we observe the image on a plane whereas the

points in the field are brought to focus on a parabolic surface. Such a surface is called Petzval surface. If we observe the expression for field curvature in the aberration function, $_2a_{20}h'^2r^2$ we can see the term r^2 ,which is the term for defocus. So field curvature is defocus but only it is multiplied by h'^2 . Unlike defocus, field curvature depends on the off axis distance and as in astigmatism, its severity grows as the square of the off axis distance. At the center however this aberration is absent. Field Curvature is intuitively defocus but parabolic with respect to the off axis distance.

3.2.6 Distortion

Distortion aberration renders the image as depicted in the Fig. 3.5. The expression for distortion $_3a_{11}h'^3r\cos\theta$ contains the term r in first degree. This is really Tilt aberration but multiplied by the third power of off axis distance h' . We can deduce that the aberration is absent at the center, as we can see from the figure below.

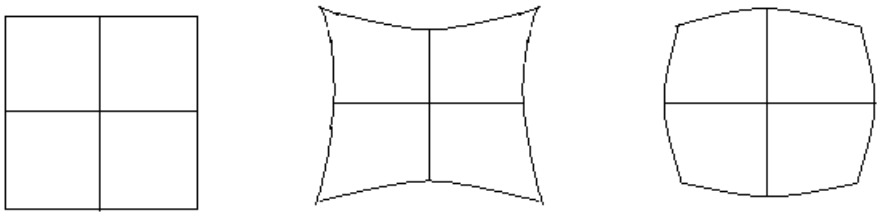

Figure 3.5: Effects of distortion

The Tilt gets more pronounced as we move away from the axis. The severity of aberration increases in third power of the off axis distance and is linear in pupil coordinates.

Chapter 4

Seidel aberrations and coefficients

In the last chapter we looked at five primary aberrations of an optical system. Now we discuss more about how they are measured and determined. We will talk about aberration coefficients and take up an example of thin lens and give the expression for calculating aberration coefficients for it. For illustrations refer [3, 2].

4.1 Quantifying primary aberrations

Wavefront propagating through an optical system does not undergo any change after it crosses the exit pupil. Theoretically, the film or sensor could serve as exit pupil too. We have defined exit pupil as the image of aperture stop as seen from the image space of the optical system. For our purposes exit pupil is a plane and we assume circular symmetry. It has

been said that wavefront at the exit pupil is spherical for an ideal image forming system. So applying our definition of aberration, we shall say that any wavefront which is either not spherical at the pupil or has a different radius of curvature is said to be aberrated.

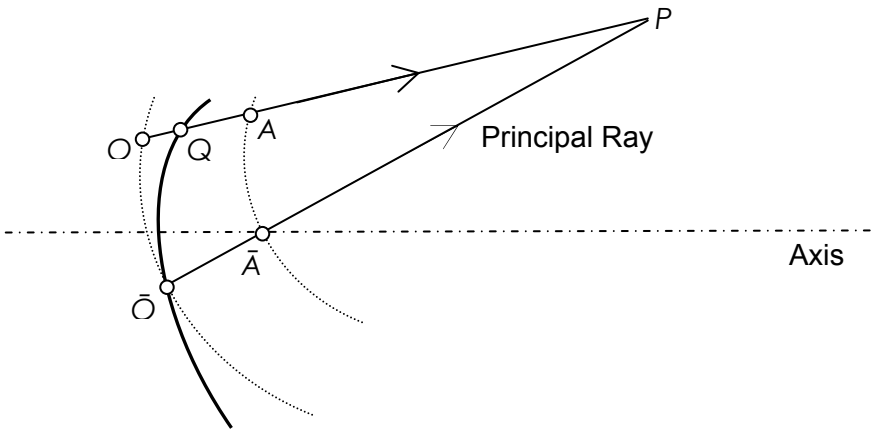

Figure 4.1: Showing wavefront propagation at pupil

Aberration is measured as the total optical path difference between a reference sphere and the aberrated wavefront across the pupil. It is measured in fractions of the wavelength λ as we are measuring path difference. For example a point object at a certain location may cause spherical aberration of 0.89 λ. It means that all rays originated at the point object and propagating through the system result in a total optical path difference of 90% of wavelength.

Optical path difference could be either positive or negative. If positive, then the aberrated rays travel longer than they should and opposite for negative aberration. Conceptually, Point Spread Function is similar to impulse response of a linear system. An aberrated optical system is not space invariant. Hence a point object, depending on its location, in the field of view gives a unique output (or an image in our case). Every point object in the field forms a unique wavefront at the exit

pupil. According to Gaussian imaging model the wavefront at the exit pupil is spherical.

In case of aberrated imaging systems the wavefront formed will not be spherical. The difference between an aberrated wavefront and the reference sphere is the Optical Path Difference for example *OQ* in Fig. 4.1 above. The total wave aberration is the sum of such path differences across the wavefront.

4.2 Seidel sums

4.2.1 General case

Aberrations are a property of each refracting surface in the optical system. The total aberration for the entire system is the sum of aberrations due to each surface. These expressions were derived by Ludwig von Seidel and hence bear his name. They are as follows (Eq. 4.1):

$$\left.\begin{aligned} S_{\mathrm{I}} &= -\sum A^2 h\Delta\left(\frac{u}{n}\right) \\ S_{\mathrm{II}} &= -\sum \overline{A} A h\Delta\left(\frac{u}{n}\right) \\ S_{\mathrm{III}} &= -\sum \overline{A^2} h\Delta\left(\frac{u}{n}\right) \\ S_{\mathrm{IV}} &= -\sum H^2 c\Delta\left(\frac{1}{n}\right) \\ S_{\mathrm{V}} &= -\sum\left\{\frac{\overline{A^2}}{A} h\Delta\left(\frac{u}{n}\right)+\frac{\overline{A}}{A} H^2 c\Delta\left(\frac{1}{n}\right)\right\} \end{aligned}\right\} \qquad (4.1)$$

Where, $A^2 = n^2\left(c - 1/l_1\right)^2$, $\overline{A} = n\left(c - 1/l_2\right)$, and $H = nhu$.

While actually summing over all surfaces we have to keep in mind that the angle of refraction of a surface is same as angle of incidence of the next surface and this signifies the quantity Δ in all the summations above. For a complete derivation of the above summation refer [3].

4.2.2 Special case: A thin lens

For our purpose, we assume thin lens as the optical system and hence obtain the following expressions (Eq. 4.2) which are derived in [3]:

$$\left.\begin{aligned} S_{\mathrm{I}} &= \frac{h^4K^3}{4n_0^2}\left\{\left(\frac{n}{n-1}\right)^2+\frac{n+2}{n(n-1)^2}\left(B+\frac{2(n^2-1)}{n+2}C\right)^2-\frac{n}{n+2}C^2\right\} \\ S_{\mathrm{II}} &= -\frac{h^2K^2H}{2n_0^2}\left\{\frac{n+1}{n(n-1)}B+\frac{2(n+1)}{n}C\right\} \\ S_{\mathrm{III}} &= \frac{H^2K}{n_0^2} \\ S_{\mathrm{IV}} &= \frac{H^2K}{n_0^2n} \\ S_{\mathrm{V}} &\equiv 0 \end{aligned}\right\} \qquad (4.2)$$

Where, $K = n_0(n-1)(c_1-c_2)$, power of the lens.

$B = \frac{n_0(n-1)(c_1-c_2)}{K}$ and $C = \frac{m+1}{m-1}$ are conjugate variables of the lens. $c_1 \& c_2$ are the lens curvature, and m is the transverse magnification of the lens.

4.3 Aberration coefficients and object distance

4.3.1 Spherical aberration

As we can see in the plot, aberration is very high when object is very close to the imaging system (the lens). Usually very high aberrations are encountered when objects are too close, that is, within about 10 cm from the imaging system. Spherical aberration never disappears, although there is a dip in its value. This dip was observed to move along abscissa with different focal lengths of lens. As seen below in Fig. 4.2, the aberration has a significant positive slope between 10 cm and 1 m, and this trend was quite consistent even with varying focal lengths. It remains more or less constant beyond 1 m.

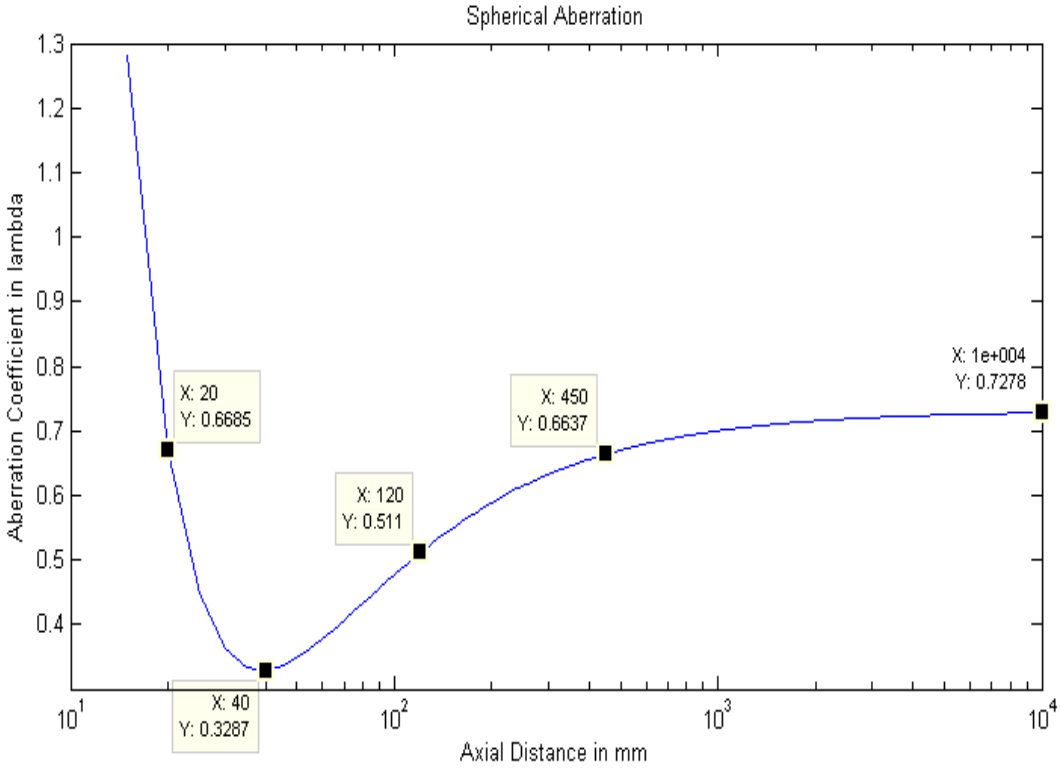

Figure 4.2: Spherical aberration vs distance

4.3.2 Coma

The plot observed is very different from that of spherical aberration. Firstly, coma increases rapidly at near distances and then settles to a constant value. One point for observation is the zero crossing of coefficient value. This is observed to shift right along abscissa with increasing focal lengths of lens. However, consistently the amount of aberration remained constant beyond 1 m. The code for plotting graphs in Fig. 4.2 & 4.3 has been included in Appendix.

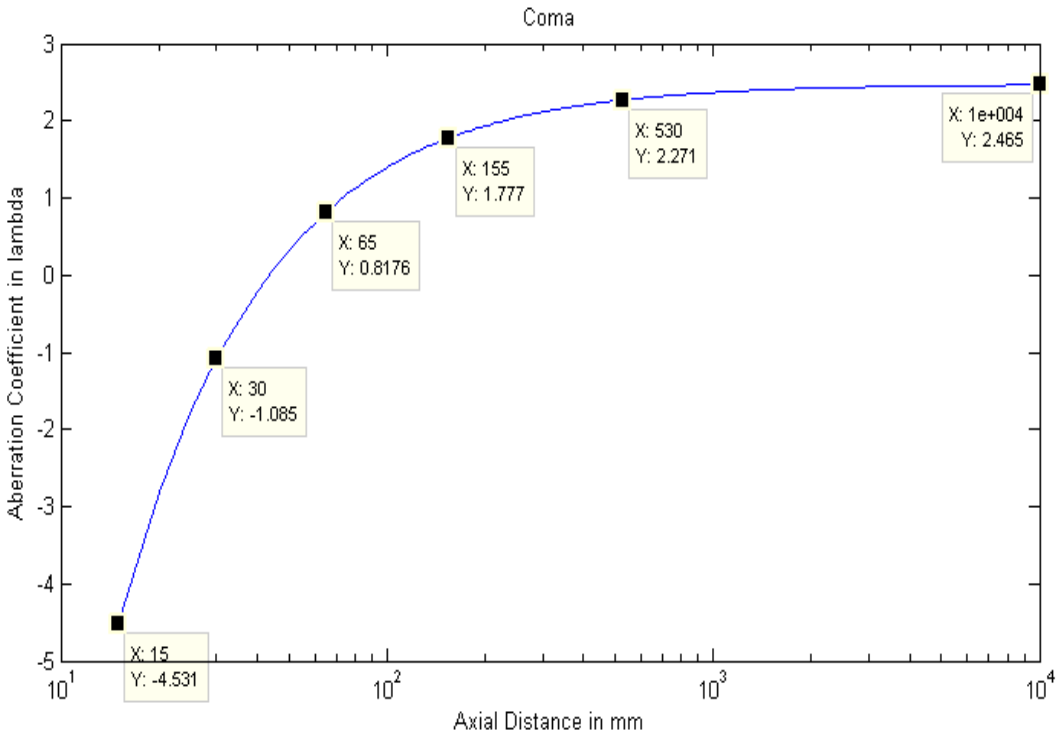

Figure 4.3: Coma vs distance

4.3.3 Other primary aberrations

Other aberrations coefficients namely, astigmatism, field curvature and distortion for a thin lens do not depend on the conjugate variable *C*. Hence it is implied that the amount of aberration doesn't depend on the

distance from the imaging system. However, in next section we will see that all five primary aberrations depend on aperture and vary exponentially with it.

4.4 Aberration coefficients and aperture

The normalized height in the pupil is a component of every aberration. It is quite obvious that aberrations depend on the size of the aperture. For example, spherical aberration varies directly as fourth power of aperture. From the graph below it is clear that as the aperture increases, aberration increases exponentially. Nature of curve obtained for all five primary aberrations were similar. The figure shows plot of spherical aberration against F Number* (aperture). Appendix contains the code to generate the graph shown in Fig. 4.4

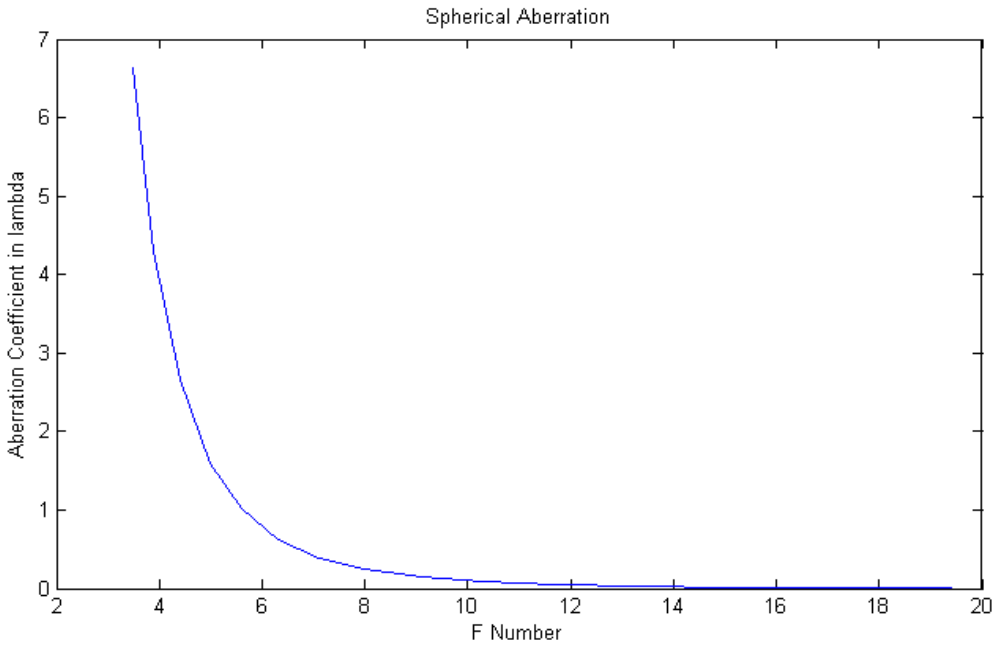

Figure 4.4: Diagram showing variation of spherical aberration coefficient against aperture

**Lower F Number means open aperture and aperture decreases as F Number increases.*

Chapter 5

Calculating aberration PSF

One of the important results of diffraction imaging model is that the Incoherent PSF is proportional to the square of the modulus of inverse Fourier Transform of the Pupil Function. We elaborate more on this result in this chapter and give a simple algorithm to calculate Incoherent PSF of an imaging system.

5.1 Background

Incoherent PSF is one which results from an object that can be divided into incoherent point sources. Pupil Function gives the complex amplitude

distribution at the exit pupil due to a point source. Its expression is given as

$$\left.\begin{aligned} P\left(\vec{r}_p;\vec{r}_o\right) &= A\left(\vec{r}_p;\vec{r}_o\right)\exp\left[ikW\left(\vec{r}_p;\vec{r}_o\right)\right] \quad \text{, in the exit pupil} \\ &= 0 \qquad\qquad\qquad\qquad\qquad\qquad\quad \text{, outside the exit pupil} \end{aligned}\right\} \tag{5.1}$$

$A\left(\vec{r}_p;\vec{r}_o\right)$ is called the apodization function and controls the amplitude distribution across the exit pupil. For our purpose it is sufficient to keep a constant value of one within a unit circle. Using the pupil function expression from Eq. 5.1 in the equation below, we can compute the PSF of the system given by Eq. 5.2.

$$PSF\left(\vec{r}_i;z_i\right) = \frac{1}{P_{ex}\lambda^2 R^2}\left|\int P\left(\vec{r}_p;z_i\right)\exp\left(-\frac{2\pi i}{\lambda R}\vec{r}_p.\vec{r}_i\right)d\vec{r}_p\right|^2 \tag{5.2}$$

For a more detailed analysis of PSF and its significance refer [5].

5.2 Algorithm to compute PSF

1. Determine the Seidel aberration coefficient (as described in the previous chapter) depending on the distance. Compute the peak aberration coefficient from the Seidel sums using the following relation.

$$\left.\begin{aligned} {}_0a_{40} &= \frac{S_{\mathrm{I}}}{8} \\ {}_1a_{31} &= \frac{S_{\mathrm{II}}}{2} \\ {}_2a_{22} &= \frac{S_{\mathrm{III}}}{2} \\ {}_2a_{20} &= \frac{S_{\mathrm{III}}+S_{\mathrm{IV}}}{4} \\ {}_3a_{11} &= S_{\mathrm{V}} \end{aligned}\right\} \tag{5.3}$$

2. Substitute aberration coefficient to obtain the aberration function,

$$W(h',r,\theta) = {}_0a_{40}r^4 + {}_1a_{31}h'r^3\cos\theta + {}_2a_{22}h'^2r^2\cos^2\theta + {}_2a_{20}h'^2r^2 + {}_3a_{11}h'^3r\cos\theta \quad (5.4)$$

3. Evaluate the aberration function using the following substitutions within a unit circle bounded by $|r| \le 1$.

$$r^2 = \frac{(x_p + y_p)^2}{h_p{}^2}\ , r\cos\theta = y_p \text{ and } h'^2 = \frac{(X_i + Y_i)^2}{h_i^2} \quad (5.5)$$

4. Use aberration function to evaluate complex amplitude at the exit pupil within the unit circle. The next section elaborates on sampling this unit circle.
5. Once complex amplitude is obtained, take Fourier Transform and square it at every sample. (According to the relation between PSF and Pupil Function)
6. Divide the PSF by total power in the pupil and normalize it to contain unit energy.

5.3 Sampling the PSF

A crucial step in calculating a PSF is the evaluation of complex amplitude at the exit pupil. Sampling, while evaluating the complex amplitude, is dividing this unit circle into squares at suitable distance. We assume that the pupil is circular and normalize its height to unity, that is, pupil will have unit radius. When we compute the complex amplitude and take its Fourier Transform, we keep the sampling rate same. Hence, to be correct physically, the sampling interval of the unit circle should be same as the sampling interval of the image (size and spacing between sensors). We can clearly see that the sampling rate depends on the resolution of the system under consideration. While calculating the PSF, sampling matrices always had radix 2 orders so that it is straightforward to compute Fast Fourier Transform. However, it was also noted, in our experiments carried out at different sampling rates that the PSF generated at lower sampling

rate (less PSF size) was not much different from PSF generated at higher sampling rate, refer Table 5.1. The error between PSFs obtained at different sampling rate was found using the error criterion is given by Eq. 5.5.

$$\varepsilon = \sum\sum\left[PSF_{\langle i \rangle}(m,n) - PSF_{\langle j \rangle}(m,n) \right]^2 \tag{5.5}$$

Where, $\langle i \rangle$ and $\langle j \rangle$ indicate the sampling rate.

	16 x 16	**32 *x* 32**	**64 x 64**	**128 x 128**	**256 x 256**	**512 x 512**
16 x 16	-	1.5331e-3	2.6895e-3	3.2201e-3	3.4880e-3	3.6331e-3
32 x 32	1.5331e-3	-	1.8374e-4	3.5156e-4	4.4955e-4	5.0551e-4
64 x 64	2.6895e-3	1.8374e-4	-	3.0723e-5	6.9239e-5	9.6748e-5
128 x 128	3.2201e-3	3.5156e-4	3.0723e-5	-	8.5671e-6	2.0657e-5
256 x 256	3.4880e-3	4.4955e-4	6.9239e-5	8.5671e-6	-	2.6875e-6
512 x 512	3.6331e-3	5.0551e-4	9.6748e-5	2.0657e-5	2.6875e-6	-

Table 5.1: Error (ε) between PSFs at different sampling rates.

In generating the error metric table, PSFs with larger than [16 x 16] samples were truncated to contain only the center [16 x 16] values. The truncated PSF was normalized and then it was used in the error metric equation shown above. It was also noted that the computation time increases by a factor of 4 as we increase the sampling rate in powers of two.

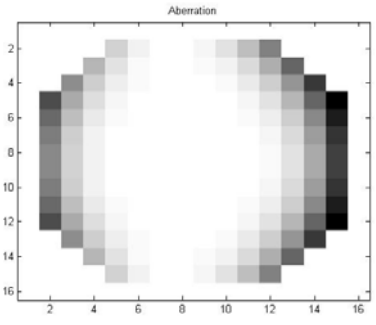

Figure 5.1 (a)

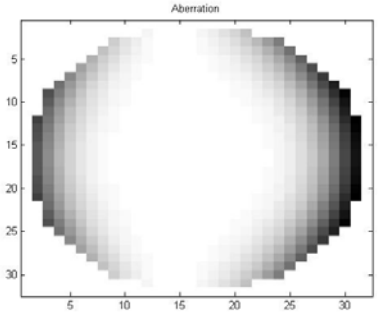

Figure 5.1 (b)

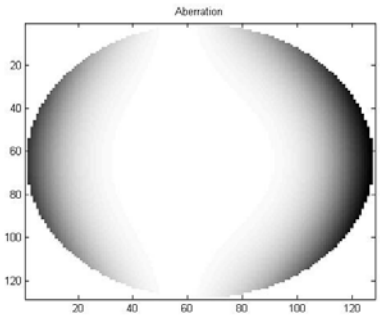

Figure 5.1 (c)

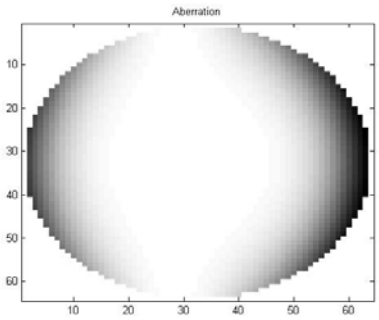

Figure 5.1 (d)

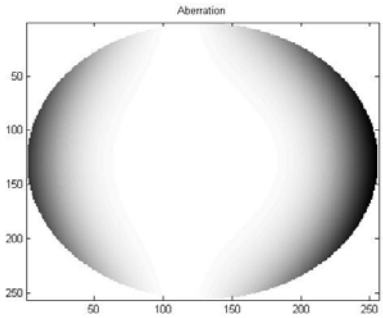

Figure 5.1 (e)

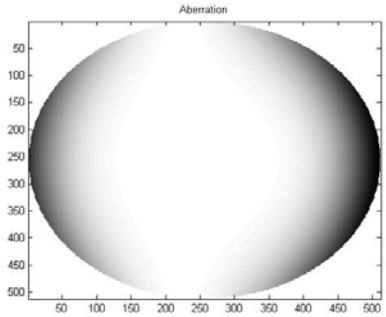

Figure 5.1 (f)

Figure 5.1 (a)-(f) Showing pupil functions sampled at different sampling rates, from 16x16 to 512x512

5.4 Some PSF examples

This section shows examples of aberration PSFs. All the PSFs have been generated using the algorithm presented before at 64x64 sampling rate. For uniformity, all the aberration coefficients have been kept constant at 1λ. All the PSFs have been generated at a point object located at (100, 100) in a 256 x 256 image. Refer [5, 6 and 10] for more regarding computation of PSF.

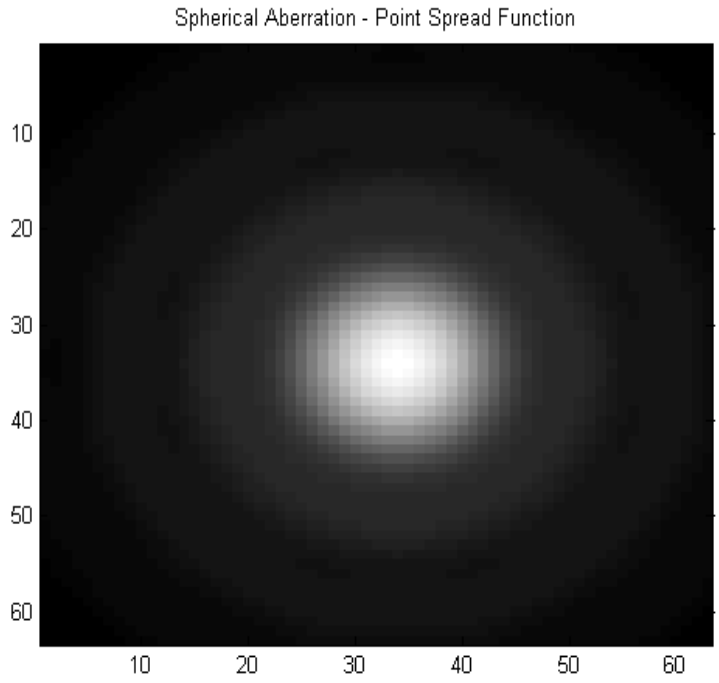

Figure 5.2: Showing spherical aberration PSF

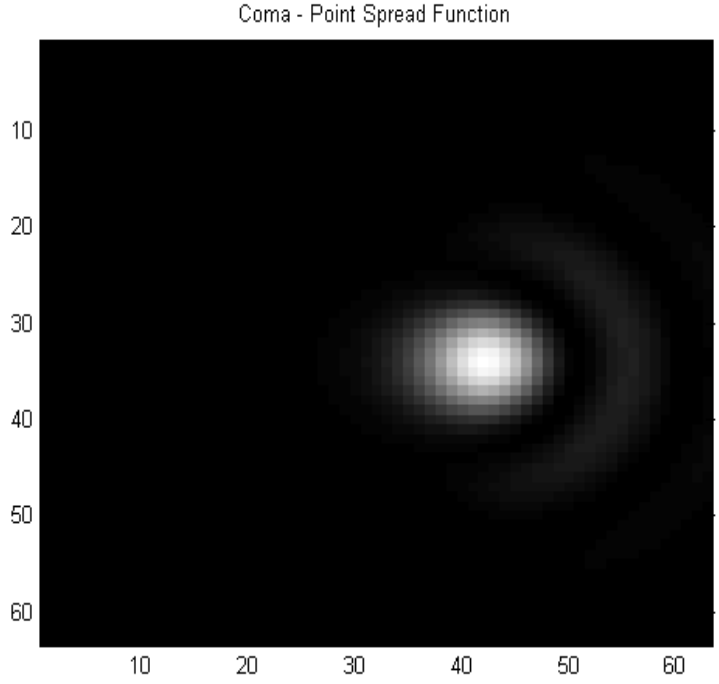

Figure 5.3: Showing coma PSF

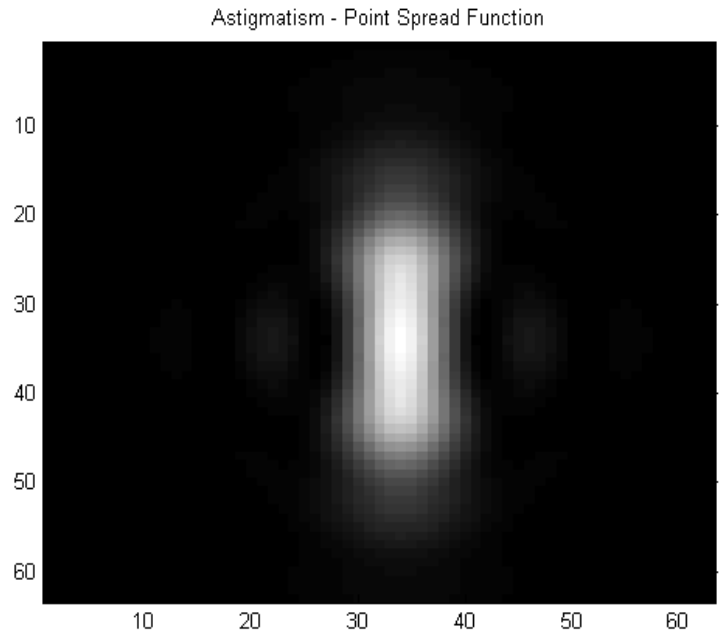

Figure 5.4: Showing astigmatism PSF

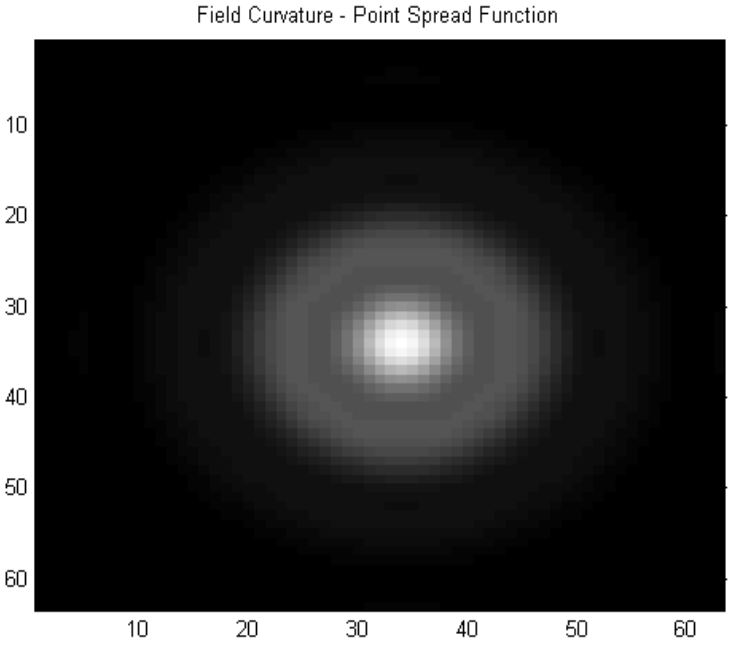

Figure 5.5: Showing field curvature (defocus) PSF

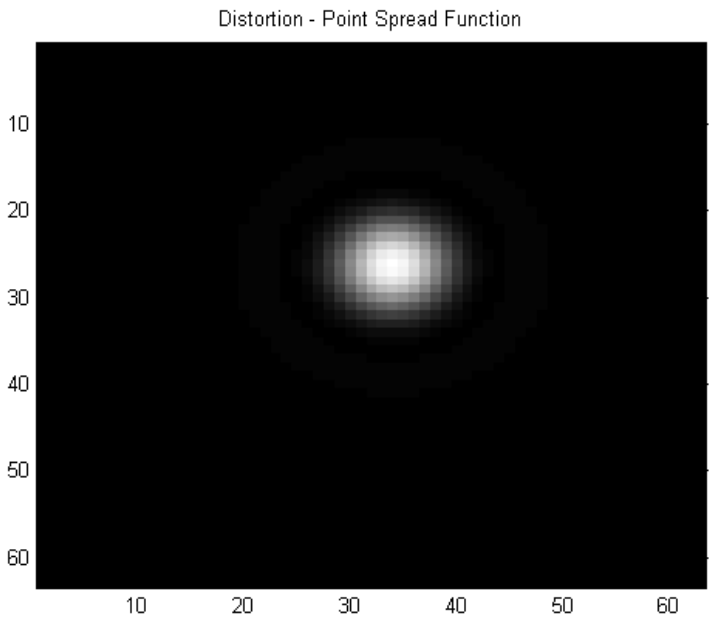

Figure 5.6: Showing distortion (Tilt) PSF

Chapter 6

Simulation of blurring using aberration PSF

So far we have discussed various topics related to aberrations and understood the behavior of each aberration. In this chapter, we will use planar images to see how each aberration affects them. Before delving into simulation a brief introduction on image blurring is given using linear system theory.

6.1 Forward blurring process

The simple relation between a blurred and a focused image is given as

$$g(x,y) = H\left[f(x,y) \right] + \eta(x,y) \qquad (6.1)$$

Here, $g(x,y)$ is the blurred image, $f(x,y)$ is the focused image, $\eta(x,y)$ is random noise and $H[\ ]$ is the linear operator. If $\eta(x,y)=0$, using superposition theorem, this equation can be written as in Eq. 6.2. It denotes the blurring of an incoherent object discussed in earlier chapters.

$$g(x,y)=\int_{-\infty}^{\infty}\int_{-\infty}^{\infty} f(\alpha,\beta)H\left[\delta(x-\alpha,y-\beta)\right]d\alpha d\beta. \qquad (6.2)$$

Analyzing Eq. 6.2, we can note that the linear operator is input with Dirac delta or the point object function. Hence the term $H\left[\delta(x-\alpha,y-\beta)\right]$ is the impulse response of the system. Since the input is a point object, it is also known as the point spread function. From the previous chapter, this theory is in agreement with shift variant imaging, as we supply point objects located at different coordinates on the image to obtain different PSFs. By writing the impulse response as $h(x,\alpha,y,\beta)$, forward blurring process hence becomes the Fredholm integral of the first kind, given in Eq. 6.3.

$$g(x,y)=\int_{-\infty}^{\infty}\int_{-\infty}^{\infty} f(\alpha,\beta)h(x,\alpha,y,\beta)\,d\alpha d\beta. \qquad (6.3)$$

A good introduction to this topic is given in [1]. Code for simulating shift variant blurring has been included in the Appendix.

6.2 Simulation

For simulation the test data has been generated by capturing images of a planar object at a distance between 1-3 m. Our assumption is that the captured image is completely focused and simulation is carried out on them to view blurring. There are two different images. Each is a grayscale image of size 640x480 pixels.

6.2.1 Case 1 - Alphabet image

In this section we will discuss the blurring simulation carried out on one of our test images called the alphabet image. The image was taken with the equipments in our lab. All the images are scaled to 40% of their original size of 640x480 pixels. As we can see from Fig. 6.1 (a), in the original gray scale image, all parts of the image are in focus and the object plane is perpendicular to the optical axis of the imaging system.

The image has been blurred with spherical aberration PSF with aberration coefficient 1. Fig. 6.1 (b) shows the results. We can observe that the bur is constant across all points and present even at the center. Hence, spherical aberration can act as shift invariant for planar objects perpendicular to the optical axis.

Figure 6.1(a)

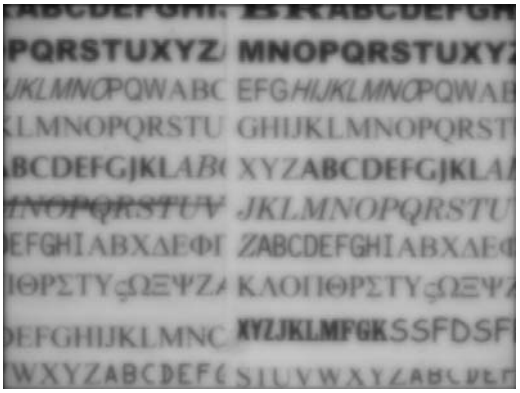

Figure 6.1(b)

Figure 6.1(a) – (b) Showing the original image and effects of spherical aberration on it

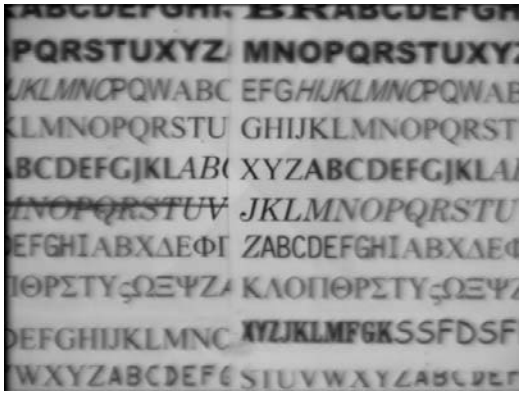

Figure 6.1(c)

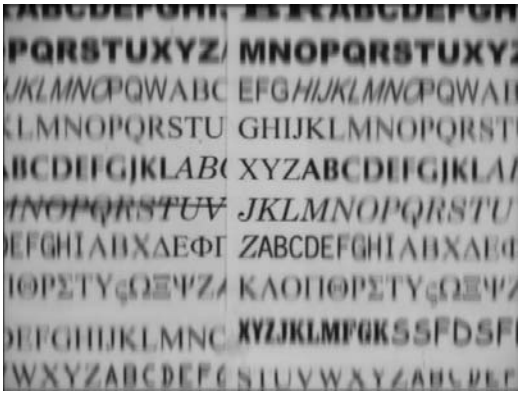

Figure 6.1(d)

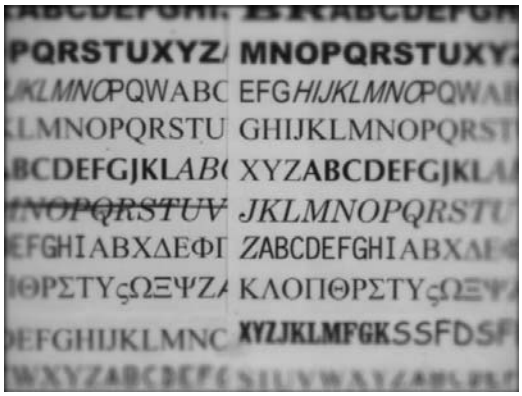

Figure 6.1(e)

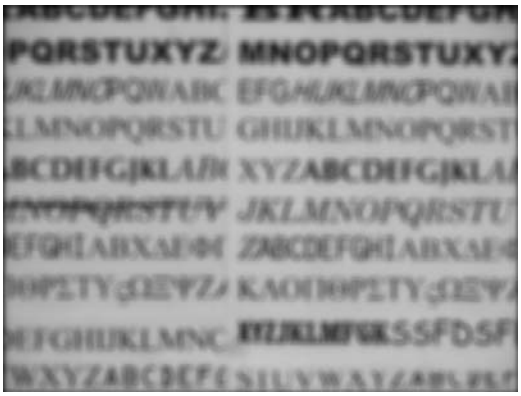

Figure 6.1(f)

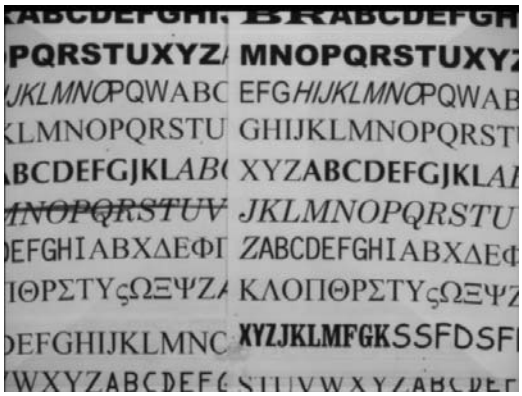

Figure 6.1(g)

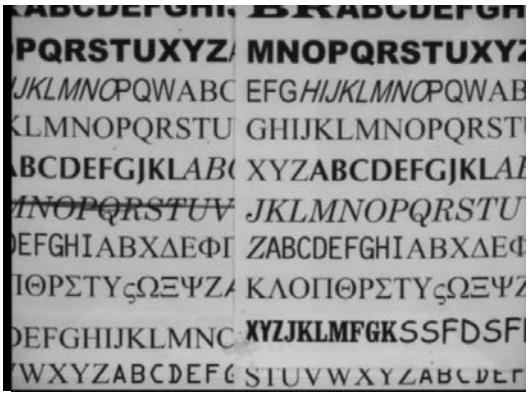

Figure 6.1(h)

Figure 6.1(c) – (h) Showing the effects of Coma, Astigmatism Field Curvature, Defocus, Barrel Distortion and Pincushion Distortion aberrations on test image in Fig. 6.1 (a)

Fig. 6.1 (c) shows blurring with coma PSF with aberration coefficient 1.5. We can distinctly observe the absence of blur near the center and its presence growing as we move away from the center. In practice coma varies directly as the distance (normalized) from the center. Also another characteristic of coma is that due to blur the features in image appear stretched.

Effects of astigmatism can be seen in Fig. 6.1(d). The letters appear stretched in the vertical direction (horizontal edge blur) and blurring is less severe in the horizontal direction. Astigmatism unlike coma varies as the square of the normalized distance from the center.

Field curvature and defocus are shown in Fig. 6.1(e) & (f) respectively. We have told earlier that field curvature is similar in nature to defocus. These two figures show clearly that defocus is constant across the image whereas field curvature varies as the square of the normalized distance from center. Hence, defocus becomes shift invariant and field curvature is not, for a planar object. The coefficient of aberration is 1.

Lastly, Fig. 6.1 (g) & (h) show simulation results with distortion PSF. An aberration coefficient of -2 and 1 was assumed for the two cases. Negative value results in a barrel distortion and pin-cushion distortion otherwise. We can see that the shape of the planar image is altered in both the cases and is similar to the conceptual figure, Fig. 3.5 of Chapter 3.

6.2.2 Case 2 – Alphabet background image

This section contains simulation results of another test image. The image is a combination of alphabets and a background containing smooth variations of intensity, as shown in Fig. 6.2 (a). The simulation of blurring using aberration PSF is shown in Fig. 6.2 (b)-(f)

Figure 6.2(a)

Figure 6.2(b)

Figure 6.2(c)

Figure 6.2(d)

Figure 6.2(e)

Figure 6.2(f)

Figure 6.2(a) Showing Alphabet background image.

Figure 6.2(b) - (f) Showing the effects of Spherical, Coma, Astigmatism Field Curvature, Defocus, Barrel Distortion and Pincushion Distortion aberrations on test image in Fig. 6.2 (a)

6.3 Variation of PSF across the image

This section pictorially shows how PSFs for different aberrations vary with the normalized radial distance from the center (image height).

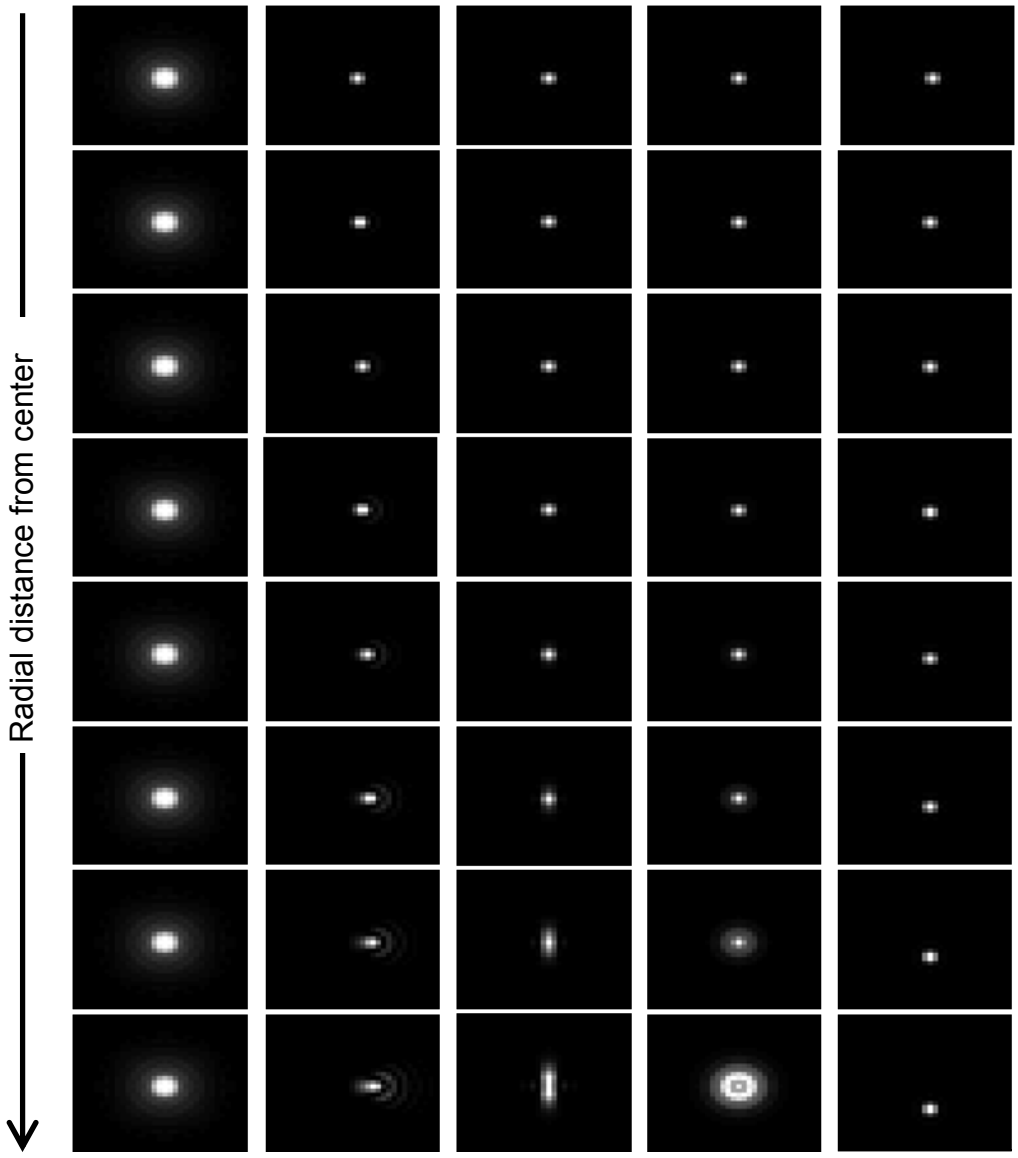

Figure 6.3: Shows five aberration-PSFs column wise left to right, Spherical, Coma, Astigmatism, Field Curvature and distortion sampled at incremental radial distance from the center. The radial distance increases by 16/128 between each PSF.

We can see from Fig 6.3 first column that spherical aberration PSFs do not vary with radial distance. From second column onwards coma, astigmatism, field curvature and distortion have been drawn. We can observe that the PSF for coma and astigmatism spread more with image height. The width of PSF grows linearly for coma but we can see from the last three images that a sudden increase in width of astigmatism PSF is present. This verifies the square relation between astigmatism and image height. The brightest spot in coma PSF moves as we move away from the axis whereas for astigmatism, only the spread is present.

Field curvature varies exactly same as astigmatism with respect to image height. This can be seen in column four of Fig. 6.3. Distortion, shown in the last column of Fig. 6.3 does not change its size but moves away from the center and this shift from center is proportional to image height in third power. This shift can be observed in the last three images of distortion PSFs.

Chapter 7

Future work

So far we have studied various aberrations focusing on the five primary aberrations. We have dealt with the phenomenon of aberrations from a physical optics perspective and taken results from diffraction imaging model. Also measurement and computation of aberration PSF was given for a simplified model of thin lens. Lastly, a simulation of degradation of images in presence of aberration was discussed.

We have learnt how primary aberrations differ from defocus. It was also observed that for aberrations like astigmatism, coma and distortion, the PSF is often not radially symmetrical. In such cases an assumption of radially symmetrical PSFs like Gaussian may not be optimal for restoration.

Another important issue addressed was the relation between depth and the aberration coefficients. We used relations derived in optics to calculate aberration coefficients and used them along with the aberration function to obtain PSF. It forms a link between PSF and depth or field of view more generally. This could help us retrieve depth information of the scene. Our future work will focus mainly on two things:

- Restoration of images degraded with aberrations;
- Investigating a possibility of recovering depth related information from aberration coefficients.

References

1. Gonzalez, Rafael C. and Woods, Richard E. *Digital Image Processing* 2007, Pearson Prentice Hall.
2. Born, M. and Wolf, E. *Principles of Optics* 1975, 5th Ed. Imprint, Oxford Pergamon Press, New York.
3. Welford, W. T *Aberrations of Symmetrical Optical Systems* 1974 Academic Press, London.
4. Gaskill, Jack D. *Linear systems, Fourier transforms, and Optics,* 1978 Wiley, New York.
5. Mahajan, Virendra N. *Optical Imaging and Aberrations - Part II* 1998 SPIE Engineering Press, Bellingham.
6. Wyant, James C. and Creath K. *Applied Optics and Optical Engineering*, Vol. XI , 1992 Academic Press.
7. Pedrotti, Frank L. and Pedrotti, Leno M. *Introduction to Optics,* 1993 2nd Ed. Prentice Hall, Englewood Cliffs, N.J.
8. Goodman, Joseph W. *Introduction to Fourier Optics* 1996 2nd Ed. McGraw Hill, New York.

9. Smith, Warren J. *Modern Optical Engineering,* 1990 McGraw Hill, New York.
10. Mahajan, Virendra N. *Zernike Circle Polynomials and Optical Aberrations of Systems with Circular Pupils*, *in Engineering and Laboratory Notes,* Applied Optics Dec. 1994.
11. Gopal, S. *Three-Dimensional Scene Recovery from Image Defocus*, Dept. of Electrical Engineering, SUNY at Stony Brook, Dec. 1994.
12. M. Subbarao, Y. Kang, S. Dutta, and X. Tu, *Localized and Computationally Efficient Approach to Shift-variant Image Deblurring*, International Conference on Image Processing, San Diego, Oct. 2008.
13. Thomas P. Costello, Wasfy B. Mikhael. *Efficient restoration of space-variant blurs from physical optics by sectioning with modified Wiener filtering,* Digital Signal Processing 13 (2003) 1-22.
14. Hazra, L.N. and Delisle, C. A. *Primary aberrations of a thin lens with different object and image space media,* J. Opt. Soc. Am. A Vol 15, No.4 April 1998.
15. Weisstein, Eric W. *Zernike Polynomial. From MathWorld--A Wolfram Web Resource*.
http://mathworld.wolfram.com/ZernikePolynomial.html
16. Sacek, V. *Notes on Telescope Optics* July 2006 Web-published http://www.telescope-optics.net/index.htm

Appendix

```
%%%%%%%%%%%%%%%%%%%%%%%%%%%%%%%%%%%%%%%%%%%%%%%%%%%%%%%%%%%%%%%%%%%%%%
%%%%%%%%%%%
%%% Calculation of Seidel Aberration Coefficients for a Thin Lens
%%%
%%% Plots aberration coefficient against object distance
%%%
%%% Shekhar Sastry, CV Lab, Stony Brook University-EE,Feb09.
%%%
%%%%%%%%%%%%%%%%%%%%%%%%%%%%%%%%%%%%%%%%%%%%%%%%%%%%%%%%%%%%%%%%%%%%%%
%%%%%%%%%%%

% Symbols
% S1, S2, S3, S4 , S5....Seidel aberration sums
% K .....................Power of thin lens
% B .....................Shape factor of lens
% C .....................Conjugate variable of lens
% H .....................Lagrange invariant
% c1,c2 .................Curvatures of surface(s)
% n .....................Refractive index
% m .....................Magnification of lens
% u .....................Angles of incidence and refraction (of
lens)
% h .....................Height of ray (usually radius of
aperture)

% Refer pp 192-193 Aberrations of Symmetrical Optical Systems by
Welford,WT
% for formuals of Seidel sums
```

```
%%%%%%%%%%%%%%%%%%%%%%%%%%%%%%%%%%%%%%%%%%%%%%%%%%%%%%%%%%%%%%%%%
%%%%%%%%%%
% Sample lens data
n = 1.6;
lambda = 5 * 10^-4; % wavelength of green in mm
delta = 0.5; % inmm

c1 = 0.02; % 1/R1 in per mm
c2 = -0.04; % 1/R2 in per mm

f = 1/((n - 1)*(c1 - c2)) % mm
ap = 4; % in mm
h = ap/2; % in mm

K = (n - 1)* (c1 - c2); % per mm
B = (c1 + c2) /(c1 - c2); % no dimension

u = atan(h/f); % thin lens approximation for field angle

H = n*h*u; % lagrange invariant (has dimension mm)

% C = m+1/(m-1)...m = f/(f - z) has no dimension

%%%%%%%%%%%%%%%%%%%%%%%%%%%%%%%%%%%%%%%%%%%%%%%%%%%%%%%%%%%%%%%%%
%%%%%%%%%%
%%%%%% ALL aberrations calculated will have dimension
millimeters(mm) %%%%%
%%%%%%%%%%%%%%%%%%%%%%%%%%%%%%%%%%%%%%%%%%%%%%%%%%%%%%%%%%%%%%%%%
%%%%%%%%%%

%SPHERICAL
S_1 = [];
st1 = (n/(n-1))^2;
st2 = (n+1)/(n*(n-1)) * B;
st3 = 2*(n+1)/n ;

% COMA
S_2 = [];
ct1 = st2;

% ASTIGMATISM AND F. CURVATURE
S_3 = [];
S_4 = [];


%####################  Varying distance from the lens
#####################

for z = 15:5:10000

%     ss = 1/z
    C = (2*f - z)/( z + delta); %delta is added to avoid division
by zero
```

```
%----------------------------------Spherical----------------------
----------
    st2 = ((n+2)/(n*(n-1)^2))*(B + 2*(n^2 - 1)*C/(n + 2))^2;
    st3 = ((n/(n+2))*C^2);
    S1 = (h^4/4) * K^3 * ( st1 + st2 - st3);
    S_1 = [S_1;S1];
%-----------------------------------------------------------------
----------

%------------------------------------Coma-------------------------
----------
    ct2 = 2*((n+1)/n) * C;
    S2 = -(h^2/2) * K^2 * H * ( ct1 + ct2 );
    S_2 = [S_2;S2];
%-----------------------------------------------------------------
----------

%------------------------------Astig'sm & F Curv------------------
----------
    S3 = K * H^2;
    S_3 = [S_3;S3];
    S_4 = [S_4;(S3/n)];
%-----------------------------------------------------------------
----------

end


%%%%%%%%%%%%%%%%%%%%%%%%%%%%%%%%%%%%%%%%%%%%%%%%%%%%%%%%%%%%%%%%%
%%%%%%%%%%
%%%%%%%%%     To convert from millimeter into units of lambda
%%%%%%%%
%%%%%%%%%%%%%%%%%%%%%%%%%%%%%%%%%%%%%%%%%%%%%%%%%%%%%%%%%%%%%%%%%
%%%%%%%%%%
S_11 = S_1/lambda;
S_21 = S_2/lambda;
S_31 = S_3/lambda;
S_41 = S_4/lambda;

% To obtain coefficients for aberration function e.g., 0a40 =
S_11/8
S_11 = S_11/8;
S_21 = S_21/2;
S_41 = (S_41 + S_31)/4;
S_31 = S_31/2;


figure;semilogx(15:5:10000, S_11);title('Spherical
Aberration');xlabel('Axial Distance in mm');ylabel('Aberration
Coefficient in lambda');
figure;stem(15:5:10000, S_11);title('Spherical
Aberration');xlabel('Axial Distance in mm');ylabel('Aberration
Coefficient in lambda');
figure;semilogx(15:5:10000, S_21);title('Coma');xlabel('Axial
Distance in mm');ylabel('Aberration Coefficient in lambda');
```

```
figure;plot(15:5:10000, S_21);title('Coma');xlabel('Axial
Distance in mm');ylabel('Aberration Coefficient in lambda');

%END
```

```
%%%%%%%%%%%%%%%%%%%%%%%%%%%%%%%%%%%%%%%%%%%%%%%%%%%%%%%%%%%%%%%%%%%%%%%%%%%%%%%%%%%%
%%%%%%%%%%
%%% Calculation of Seidel Aberration Coefficients for a Thin Lens
%%%
%%% Plots aberration coefficient against aperture (F Number)
%%%
%%% S Sastry, Computer Vision Lab, Stony Brook University-
EE,Feb09.     %%%
%%%%%%%%%%%%%%%%%%%%%%%%%%%%%%%%%%%%%%%%%%%%%%%%%%%%%%%%%%%%%%%%%%%%%%%%%%%%%%%%%%%%
%%%%%%%%%%

% Symbols
% S1, S2, S3, S4 , S5....Seidel aberration sums
% K .....................Power of thin lens
% B .....................Shape factor of lens
% C .....................Conjugate variable of lens
% H .....................Lagrange invariant
% c1,c2 .................Curvatures of surface(s)
% n .....................Refractive index
% m .....................Magnification of lens
% u .....................Angles of incidence and refraction (of
lens)
% h .....................Height of ray (usually radius of
aperture)

% Refer pp 192-193 Aberrations of Symmetrical Optical Systems by
Welford,WT
% for formulas of Seidel sums

%%%%%%%%%%%%%%%%%%%%%%%%%%%%%%%%%%%%%%%%%%%%%%%%%%%%%%%%%%%%%%%%%%%%%%%%%%%%%%%%%%%%
%%%%%%%%%%
% Sample lens data
n = 1.6;
lambda = 5 * 10^-4; % wavelength of green in mm
delta = 0.5; % in mm

c1 = 0.02; % 1/R1 in per mm
c2 = -0.04; % 1/R2 in per mm

f = 1/((n - 1)*(c1 - c2)) % mm

K = (n - 1)* (c1 - c2); % per mm
B = (c1 + c2) /(c1 - c2); % no dimension

z  = 78;  % in mm
% C = m+1/(m-1)...m = f/(f - z) has no dimension
C = (2*f - z)/( z + delta); %delta is added to avoid division by
zero
%%%%%%%%%%%%%%%%%%%%%%%%%%%%%%%%%%%%%%%%%%%%%%%%%%%%%%%%%%%%%%%%%%%%%%%%%%%%%%%%%%%%
%%%%%%%%%%
%%%%%% ALL aberrations calculated will have dimension
millimeters(mm) %%%%%
%%%%%%%%%%%%%%%%%%%%%%%%%%%%%%%%%%%%%%%%%%%%%%%%%%%%%%%%%%%%%%%%%%%%%%%%%%%%%%%%%%%%
%%%%%%%%%%

%SPHERICAL
```

```
S_1 = [];
st1 = (n/(n-1))^2;
st2 = (n+1)/(n*(n-1)) * B;
st3 = 2*(n+1)/n ;

% COMA
S_2 = [];
ct1 = st2;

% ASTIGMATISM AND F. CURVATURE
S_3 = [];
S_4 = [];

%####################  Varying aperture of the lens
####################
fn = 3.5; % starting aperture
fn_k = ( sqrt(2) - 1 ) / 3; % Calculating F Number

A_P = [];
F_N = [];
for no = 1 : 15

    ap = f / fn ; % in mm
    A_P = [A_P; ap];
    F_N = [F_N; fn];

    h = ap/2; % in mm
    u = atan(h/f); % thin lens approximation for field angle
    H = n * h * u; % lagrange invariant (has dimension mm)

%---------------------------------Spherical----------------------
----------
    st2 = ((n+2)/(n*(n-1)^2))*(B + 2*(n^2 - 1)*C/(n + 2))^2;
    st3 = ((n/(n+2))*C^2);
    S1 = (h^4/4) * K^3 * ( st1 + st2 - st3);
    S_1 = [S_1;S1];
%------------------------------------------------------------------
----------

%-----------------------------------Coma-----------------------
----------
    ct2 = 2*((n+1)/n) * C;
    S2 = -(h^2/2) * K^2 * H * ( ct1 + ct2 );
    S_2 = [S_2;S2];
%------------------------------------------------------------------
----------

%----------------------------Astig'sm & F Curv-----------------
----------
    S3 = K * H^2;
    S_3 = [S_3;S3];
    S_4 = [S_4;(S3/n)];
%------------------------------------------------------------------
----------
    % Calculate next F Num
    fn = fn + fn * fn_k;
```

```
    fn = floor(fn*10) / 10; % Precision at one decimal place
end



%%%%%%%%%%%%%%%%%%%%%%%%%%%%%%%%%%%%%%%%%%%%%%%%%%%%%%%%%%%%%%%%%
%%%%%%%%%%
%%%%%%%%%     To convert from millimeter into units of lambda
%%%%%%%%
%%%%%%%%%%%%%%%%%%%%%%%%%%%%%%%%%%%%%%%%%%%%%%%%%%%%%%%%%%%%%%%%%
%%%%%%%%%%
S_11 = S_1/lambda;
S_21 = S_2/lambda;
S_31 = S_3/lambda;
S_41 = S_4/lambda;

% To obtain coefficients of aberration in aberration function W()
S_11c = S_11 / 8;
S_21c = S_21 / 2;
S_31c = S_31 / 2;
S_41c = (S_31 + S_41) / 4;

% Plot against F Number
figure;plot(F_N, S_11c);title('Spherical Aberration');xlabel('F
Number');ylabel('Aberration Coefficient in lambda');
figure;plot(F_N, S_21c);title('Coma');xlabel('F
Number');ylabel('Aberration Coefficient in lambda');
figure;plot(F_N, S_31c);title('Astigmatism');xlabel('F
Number');ylabel('Aberration Coefficient in lambda');
figure;plot(F_N, S_41c);title('Field Curvature');xlabel('F
Number');ylabel('Aberration Coefficient in lambda');

% END
```

```
%%%%Shift Variant Blurring with Primary Aberrations
% Program Description:
%
% -   Calculate different PSFs with different aberration
coefficient
%     based on the radial distance from the center (only if not
Spherical)
%
% -   Store it in a 3D matrix with primary index as the distance
from the center
%%%%%%%%%%%%%%%%%%%%%%%%%%%%%%%%%%%%%%%%%%%%%%%%%%%%%%%%%%%%%%%%%%%%
% CODE FOR THESE THREE STEPS HAVE BEEN OMITTED HERE.
%
% -   Read the image and perform shift variant blurring using
PSFs from the
%     stored array

% By Shekhar Sastry, CVL, ECE DEPT., STONY BROOK UNIVERSITY May
2009

%%%%%%%%%%%%%%%%%%%%%%%%%%%%%%%%%%%%%%%%%%%%%%%%%%%%%%%%%%%%%%%%%%%%
% Read the image and blur
%%%%%%%%%%%%%%%%%%%%%%%%%%%%%%%%%%%%%%%%%%%%%%%%%%%%%%%%%%%%%%%%%%%%

%%% PSF is stored in a 3D array called psfArr

fImg = imread('Image\Alphabet.tif'); % Input image
fImg = rgb2gray(fImg);
[imY imX] = size(fImg);

midY = floor(imY/2);
midX = floor(imX/2);
gImg = zeros(size(fImg));
gImg(1:end,1:end) = im2double(fImg);

gImgTmp = zeros(imY+32,imX+32);

% Blurring...........
for y = 17 : imY+16
    for x = 17 : imX+16

        % Logic to select the PSF based on the distance from the
center
        % Selects max(Xdistance,Ydistance) as a rule to pick PSF
        xDist = abs(floor((x - imX/2)/(imX/(2*midX))));
        yDist = abs(floor((y - imY/2)/(imY/(2*midY))));
        dist = max(xDist,yDist);
        if dist <= 0
            dist = 1;
        elseif dist > 128
            dist = 128;
        end
        % Each PSF is weighted by the intensity value and summed
up
        % Numerically computing shift variant blur (superposition
integral)
```

```
        gImgTmp((y-16):(y+16),(x-16):(x+16)) = gImgTmp((y-
16):(y+16),(x-16):(x+16)) + ( squeeze(psfArr(dist,:,:)) *
gImg((y-16),(x-16)));
    end
end

% Throwing away pixels outside the border
bImg = gImgTmp(17:imY+16,17:imX+16);

% Rescaling image to Uint8 value
b_img = uint8(255 * bImg);
imwrite(b_img,'Blurring\New\Alphabet_coma_c15.jpg','JPEG');

% END
```